American Mineralogist, Volume 91, pages 1442–1447, 2006

A neutron powder diffraction study of Fe and Ni distributions in synthetic pentlandite and violarite using ^{60}Ni isotope

CHRISTOPHE TENAILLEAU,[1,*] BARBARA ETSCHMANN,[1] RICHARD M. IBBERSON,[2] AND ALLAN PRING[1,3,†]

[1]Department of Mineralogy, South Australian Museum, North Terrace, Adelaide, South Australia 5000, Australia
[2]ISIS Facility, Rutherford Appleton Laboratory, Chilton, Didcot, Oxon OX11 0QX, U.K.
[3]Department of Geology and Geophysics, University of Adelaide, North Terrace, Adelaide, South Australia 5005, Australia

ABSTRACT

Cation ordering in two important iron nickel sulfide minerals, pentlandite and violarite, was studied by neutron powder diffraction using samples prepared with isotopically enriched ^{60}Ni. Pentlandite of composition $Fe_{4.8}Ni_{4.2}S_8$, annealed at 150° C for 1 month has a disordered Ni/Fe distribution with Ni occupying 57(2)% of the octahedral site and 46(1)% of the tetrahedral site with a unit cell repeat of 10.1075(1) Å. After annealing for a further 2 months at 150 °C the Ni/Fe distribution is still disordered with 53(2)% Ni in the octahedral site and 48(2)% Ni in the tetrahedral site and the cell parameter increased by 0.21% possibly due to slight readjustment of the Fe/Ni ratio.

Synthetic violarite, $FeNi_2S_4$, prepared at 300 °C, exhibits ordering of Ni onto the tetrahedral site, with Fe and the remaining Ni sharing the octahedral site. In situ neutron diffraction heating experiments in which pentlandite and violarite were heated up to 300 °C for 12 hours did not alter the Ni/Fe distribution between tetrahedral and octahedral sites. Violarite did not exhibit any evidence of magnetic ordering upon cooling to –173 °C. The interatomic distances in the two structures indicate that in pentlandite Fe^{2+} and Ni^{2+} are high spin and in violarite Fe^{2+} is low spin with Ni^{3+} with an inverted spinel structural type.

Keywords: Neutron diffraction, cation ordering, ^{60}Ni isotope, pentlandite, violarite, thiospinel

INTRODUCTION

Pentlandite and violarite are important iron nickel sulfides, frequently found together in mafic nickel deposits where they are usually the major ore minerals. Pentlandite is a primary mineral and usually forms as an exsolution product with pyrrhotite from the break down of the monosulfide solid solution (*mss*) (Naldrett et al. 1967; Vaughan and Craig 1974; Durazzo and Taylor 1982; Etschmann et al. 2004). Natural pentlandite shows an irreversible thermal expansion upon heating to 250 °C that is thought to be associated with the break down of Fe and Ni ordering over the tetrahedral and octahedral sites (Tsukimura 1989). Tsukimura (1989) reported that an ordered natural pentlandite $(Ni_{4.57}Fe_{4.4}Co_{0.03})S_8$ with a = 10.051 Å expanded to a = 10.108 Å after disordering by annealing at 250 °C, an expansion of 0.56%. Rajamani and Prewitt (1975) observed a similar expansion (0.55%) on disordering a slightly more Ni-rich pentlandite. Tsukimura (1989) predicted that the disordering temperature for natural pentlandite might be as low as 111 °C. Etschmann et al. (2004) found that annealing synthetic pentlandites at 150 or 200 °C for up to 5 months resulted in a contraction of the unit-cell parameter suggesting that Fe/Ni ordering might have occurred at these temperatures. Mössbauer, magnetic, and X-ray diffraction (anomalous dispersion method) measurements indicate that Fe is preferentially ordered onto the octahedral site for natural pentlandite (Knop et al. 1970; Tsukimura and Nakazawa 1984; Tsukimura 1989).

Violarite can form as a hypogene product, via exsolution from pentlandite, but is more commonly a supergene oxidation product of pentlandite (Nickel et al. 1974; Mirsa and Fleet 1974; Grguric 2002; Tenailleau et al. 2006). Violarite is a thiospinel and the Fe and Ni are distributed over tetrahedral and octahedral sites in a *ccp* array of S atoms. There are important similarities between the crystal chemistries of pentlandite and violarite: both are based on cubic close packing of S with the metal atoms distributed over octahedral and tetrahedral sites and they can accommodate variable Fe/Ni ratios. In terms of occupation of available tetrahedral and octahedral sites in the S lattice the pentlandite and violarite structures can be viewed as opposites. In pentlandite, the Fe and Ni atoms occupy ½ of the tetrahedral sites and 1/8th of the octahedral sites in the *ccp* S array (Fig. 1a), whereas in the violarite structure they occupy ½ of the octahedral and 1/8th of the tetrahedral sites (Fig. 1b).

There is considerable scope for the ordering of the Fe and Ni atoms in both structures. Ordering in spinels is well known. In normal spinels, the divalent cations occupy the octahedral site

* Present address: Laboratoire CRISMAT-UMR 6508, ENSI Caen-6, Boulevard du Marechal Juin-14050 CAEN Cedex, France
† E-mail: pring.allan@saugov.sa.gov.au

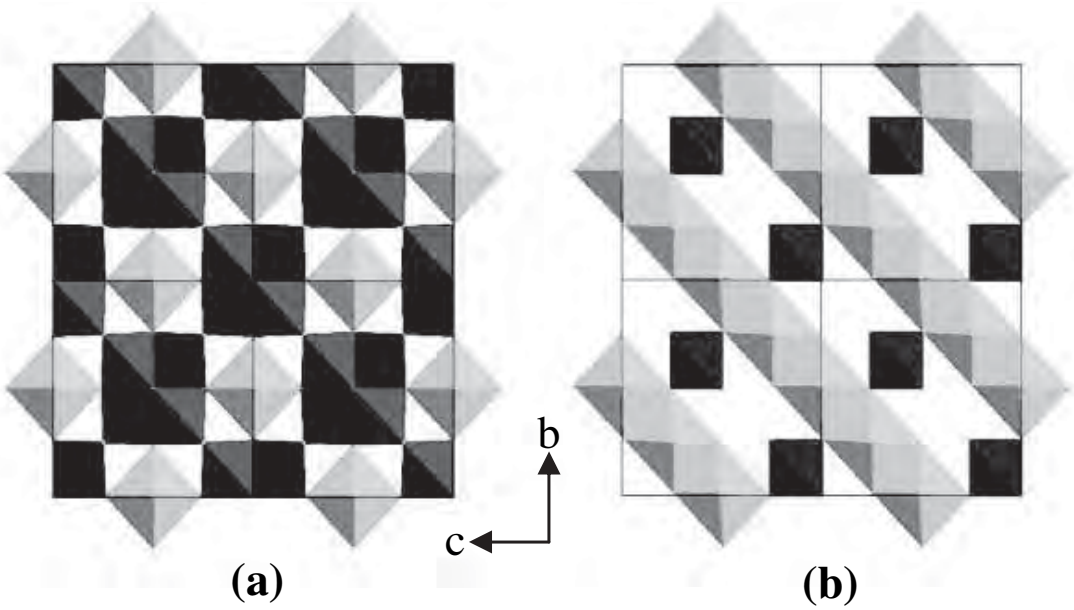

FIGURE 1. Schematic representations of the cubic (**a**) pentlandite and (**b**) violarite structures. MS_6 octahedra are gray while MS_4 tetrahedra are black.

and the trivalent cation the tetrahedral site. In inverse spinels, half of the divalent cations occupy the tetrahedral site and the other half the octahedral site, with the trivalent cations. A range of intermediate configurations is possible. From magnetic susceptibility, thermoelectric power, and Mössbauer spectroscopy measurements Townsend et al. (1977) concluded that Fe^{2+} in violarite should have delocalized electrons if it occupies the tetrahedral site or be in a localized low-spin configuration in the octahedral site. They also assigned a low-spin configuration to Ni^{3+} in the octahedral site. With Fe^{2+} in the octahedral site, violarite would have an inverted spinel structure. Vaughan and Craig (1985) suggested that violarite contains Fe in a low spin state mainly on the octahedral site but also some Fe on the tetrahedral site. Fedorov et al. (2003) presented an extensive review of the crystal chemistry of thiospinels focusing on the magnetic semiconducting thiospinels related to $CuCr_2S_4$. They reported that violarite is an inverse spinel with Fe ordered onto the octahedral sites and present both as low spin Fe^{2+} and high spin Fe^{3+}.

The detailed study of metal distribution in both pentlandite and violarite is hampered due to the similarity of the iron and nickel scattering factors for X-rays. The difference in the coherent scattering lengths of Fe and Ni for neutron scattering is only slightly greater than those in X-ray scattering curves (0.95 and 1.03×10^{-12} cm, respectively), so Fe/Ni distribution is best observed by use of ^{60}Ni (with a scattering amplitude of 0.28×10^{-12} cm) in combination with natural Fe.

EXPERIMENTAL METHODS

SYNTHESIS

Stoichiometric proportions of precisely weighed amounts of Fe (1 mm diameter wire, 99.9+%, Aldrich), Ni (1 mm diameter wire, 99+%, Aldrich), or ^{60}Ni isotope (metal powder, 99.60%, Isoflex) and S (granules, 99.99+%, Aldrich) were mixed together in silica tubes sealed under vacuum (pressure ~10^{-2} torr). Two samples of each material were prepared (pentlandite and violarite), one sample was prepared with the ^{60}Ni isotope, the other with normal Ni. Charges of approximately 3.5 g each were synthesized to satisfy the neutron diffraction requirements. Since the results for normal Ni are identical with the ^{60}Ni samples, they will not be discussed in detail in this paper.

The preparation process for pentlandite followed the method described by Etschmann et al. (2004) and involved making first *mss* of composition $Fe_{0.8}Ni_{0.2}S$. The charges were sealed under vacuum into 10 mm diameter silica tubes and were heated slowly to 300 °C, then taken up to 500 and 800 °C, soaking for 12 hours at each stage. This minimized tube failure due to high-S vapor pressure above 450 °C. The tubes were quenched in water, opened, the charges ground under acetone, and resealed in silica tubes under vacuum to ensure the homogeneity of the *mss*. The charges were then heated at 1100 °C for 2 h, cooled to 900 °C annealed for 7 days and then quenched in a large volume of cold water. This resulted in homogeneous samples with a relatively uniform 0.5 mm grain size. Quenching brought the samples from 900 °C to room temperature in less than 10 s. The sample was then annealed at 200 °C for 2 months and then quenched. The samples were then used in some preliminary neutron diffraction experiments at Lucas Heights, so before use in the current experiments they were re-homogenized by annealing at 600 °C for 24 h before cooling to150 °C and annealing for a month before quenching in cold water. At all times during heating the samples were sealed in evacuated thin-walled silica tubes.

Violarite was prepared using the two-stage method of Townsend et al. (1977), which consists of first preparing a nickel-rich *mss* and then adding extra sulfur. Charges, corresponding to a $FeNi_2S_3$ bulk composition, were heated to 300 °C, then 500 and 700 °C at 2 °C/min and held for 12 hours at each temperature to minimize tube failure due to S gas. The heating cycle was continued to 1000 °C, holding for 2 days, cooling to 900 °C and then quenching in cold water. The charges were then ground under acetone and sealed in new silica tubes under vacuum with the extra sulfur required to transform the $FeNi_2S_3$ to $FeNi_2S_4$. Samples were finally annealed for 3 weeks at 300 °C and then quenched in cold water.

Neutron diffraction at ISIS

The high-resolution powder diffractometer (HRPD) at ISIS, U.K., has three detector banks that measure simultaneously: the backscattering (Bank 1) and 90° (Bank 2) detector banks using ZnS scintillators. The third detector bank (low angle) has a ^{3}He gas tube detector [see Ibberson et al. (1992) for details]. The detectors span 2θ ranges of 160–176° (Bank 1), 80–100° (Bank 2), and 28–32° (Bank 3) with Ω(ster) of 0.41, 0.70, and 0.01 giving $\Delta d/d$ resolutions of ~4×10^{-4}, 2×10^{-3}, and 2×10^{2}, respectively. Time-of-flight data were collected in the 35–120 ms range,

corresponding to a *d*-spacing range of 0.72–2.49 Å. Data were then normalized to the incident neutron spectrum and the detector efficiency correction was made using the VA_COR program. The background and empty spectrasil tube pattern were subtracted from the data. A binning size of unity was used and no self-scattering and absorption corrections were applied.

The natural Ni- and ^{60}Ni-pentlandites that had been annealed for one month at 150 °C were both measured in sealed under vacuum spectrasil tubes for comparison using 4 and 6 hour scans at room temperature, respectively. The samples were then heated at a rate of 1 °C/min and measured for three hours at 225 °C and four hours at 300 °C. Following these experiments, the ^{60}Ni pentlandite was annealed for 2 months at 150 °C and then re-measured at room temperature on the HRPD instrument at ISIS for 6 hours.

The normal Ni- and ^{60}Ni violarites were measured in sealed spectrasil tubes for 4 hours each at room temperature for comparison. Hourly data collections were then undertaken every 75° from 75 to 300 °C with a heating rate of 2 °C/min between each step and one hour stabilization at each stage before measurement. Following these heating runs the violarite samples were cooled to room temperature and left for 12 hours before cooling down to –73 and –173 °C for 6 hour scans.

Structure refinement procedures

The data were analyzed with GSAS to determine the structural characteristics of each material and variations with temperature. The zero shift was only refined for the room temperature profile and then kept constant over the whole temperature range.

For the refinements of the mineral structures, the scale factors, background, unit-cell parameters, and peak-shape parameters (pseudo-Voigt profile function of type 2 with a 0.001 peak cutoff) were initially refined. The background was an 8 term shifted Chebyschev function and the TOF profile function of type 2 (Ikeda-Carpenter type) was used where alpha1, beta, sigma1, and gamma1 were refined until convergence was achieved. Since none of the known polytypes of pyrrhotite could be satisfactorily fitted as the second phase the simple pyrrhotite subcell of hexagonal symmetry ($P6_3/mmc$ space group) was used to model the pyrrhotite intergrowth with the pentlandite, with metal site occupancy set at the appropriate stoichiometry ($M_{7.5}S_8$). Isotropic displacement parameters for the S and cations (a single parameter for both Fe and Ni) and the atomic parameters (32*f* and 24*e* sites in pentlandite, space group $Fm\bar{3}m$ and 32*e* site in violarite, space group $Fd\bar{3}m$) were then refined. All of these latter parameters were then fixed at their final values before refining Fe/Ni distribution in the case of pentlandite samples. The Fe/Ni ratio in the pentlandite and the violarite were not fixed during the refinement. Various disordered and ordered starting models were refined but all were found to converge to the same solution.

Results and discussion

Metal distribution in pentlandite

The observed, calculated, and difference diffraction patterns for ^{60}Ni-pentlandite at 25 and 300 °C are shown in Figure 2. Detector bank 1 has the best resolution and covers a large *d*-spacing range so only these data were used in the structural refinement. These data are not affected strongly by the presence of any supercell or magnetic reflections from pyrrhotite and the simple NiAs subcell of pyrrhotite was used to successfully model the *mss*/pyrrhotite in the refinement (see Tenailleau et al. 2005 for discussion of magnetic ordering in pyrrhotites). Compositions and unit-cell parameters at 25, 225, and 300 °C are listed in Table 1 and the positional and displacement parameters are given in Table 2. The compositions for pentlandite and pyrrhotite determined from the profile refinements are in excellent agreement with those determined by electron microprobe analysis for similar specimens (Etschmann et al. 2004). Positional and displacement

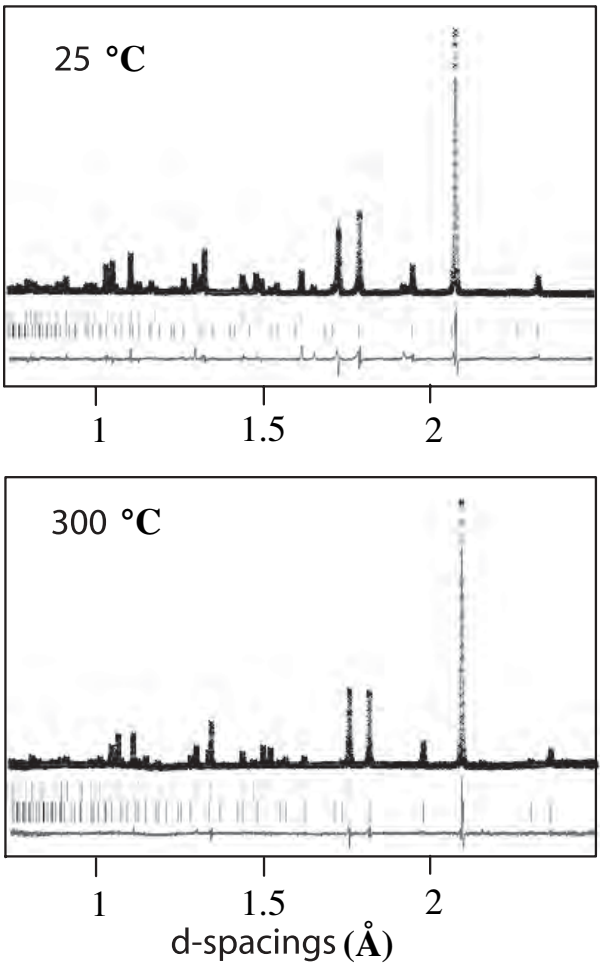

Figure 2. Observed (cross), calculated (weak line), and difference (strong bottom line) time-of-flight neutron diffraction patterns for ^{60}Ni-containing pentlandite at 25 °C (upper) and 300 °C (lower) using backscattering detectors (bank 1). Bragg peaks are represented by vertical lines: pyrrhotite (top) and pentlandite (bottom). Goodness-of-fit parameters (R_p, R_{wp}, χ^2) are: 0.1469, 0.1814, 5.355 and 0.1291, 0.1498, 2.382 at 25 and 300 °C, respectively.

Table 1. Unit-cell parameters and compositions of ^{60}Ni-pentlandite at various temperatures

T (°C)	Formula	wt%	*a* (Å)	%^{60}Ni(O)	%^{60}Ni(T)
25*	$Fe_{4.8}Ni_{4.2}S_8$	34(1)	10.1075(1)	57(2)	46(2)
225	$Fe_{4.8}Ni_{4.2}S_8$	34(1)	10.2045(1)	50(2)	47(2)
300	$Fe_{4.8}Ni_{4.2}S_8$	34(1)	10.2349(1)	50(2)	46(2)
25†	$Fe_{4.6}Ni_{4.4}S_8$	35(1)	10.1296(1)	52(2)	48(2)

Notes: Estimated standard deviations are given in brackets. T stands for tetrahedra and O for octahedra.
* Composition and unit-cell parameters for the co-existing pyrrhotite are $Fe_{6.6}Ni_{0.9}S_8$, a =3.4471(1) and c =5.7517(1) Å.
† After an additional 2 months annealing at 150 °C.

Table 2. Positional and displacement parameters of ^{60}Ni-pentlandite

T (°C)	x(M) in 32*f*	U_{iso}(M) × 10^2 (Å^2)	x(S) in 24*e*	U_{iso}(S) × 10^2 (Å^2)
25	0.1274	0.53	0.2590	0.38
225	0.1280	1.10	0.2624	0.53
300	0.1276	1.61	0.2600	0.99
25*	0.1273	0.95	0.2601	0.81

Notes: M represents the metal. Since those parameters were fixed during the final cycles of refinement (for M distribution) errors are not given here.
x(M) = y(M) = z(M) ~ 0.125 : 32*f* Wyckoff position (Tetrahedral site) for $Fm\bar{3}m$ space group
x(M) = y(M) = z(M) = 0.5 : 4*f* (Octahedral site)
y(S1) = z(S1) = 0 : 24*e*
x(S2) = 0.25 and y(S2) = z(S2) = 0 : 8*c*
* After an additional 2 months annealing at 150 °C.

parameters are shown in Table 2 and are in very good agreement with those of Rajamani and Prewitt (1973) and Tsukimura (1989). The results show that the metal distribution in pentlandite is disordered over the thermal range examined in this study; the tetrahedral and octahedral sites are each occupied by an equal mixture of Ni and Fe. This situation does not change even after an additional two months annealing at 150 °C (Table 1).

Interatomic distances and angles for the four different refinements are listed in Table 3. There is one type of short intermetallic distances, within the cubic clusters formed of eight tetrahedra, and three types of M-S shortest distances, one in octahedral environment and the other two in tetrahedral environments. Four types of M-S-M angles and two of S-M-S angles can vary with temperature. The single M-S distance within the octahedra is relatively long, 2.44(2) Å, at room temperature for ^{60}Ni-pentlandite and can be compared with those from natural ordered pentlandites where M(O)-S ~2.37 Å (Rajamani and Prewitt 1973). The short distances in natural pentlandite were originally thought to be due to ordering of Ni on the octahedral site (Rajamani and Prewitt 1975), however later work of Tsukimura and Nakazawa (1984) and Tsukimura (1989) found that Fe^{2+} is ordered onto this site. The relatively long bond distance in ^{60}Ni-pentlandite (disordered) implies high spin state Fe^{2+}, a radius of 0.78 Å compared to 0.61 Å for low spin Fe^{2+} (Shannon 1976). Ni^{2+} in an octahedral environment has a radius of 0.69 Å, while the radii for Ni^{3+} in high and low spin states are 0.60 and 0.56 Å, respectively (Shannon 1976). A low spin state for Fe^{2+} or Ni^{2+} in octahedral environment would imply a shorter M(O)-S distance [for instance, ~2.26 Å in pyrite (Rajamani and Prewitt 1973)]. The M(T)-S distance obtained for ^{60}Ni-pentlandite is also consistent with Fe^{2+} in the tetrahedral site, although the presence of clusters formed around the M(T)-M(T) bonds makes the metal environment difficult to interpret. One obvious result from the current experiment is that the Fe/Ni distribution in the synthetic pentlandite is not ordered even after annealing at 150 °C for 2 months despite the findings of Etschmann et al. (2004). In that study a marked decrease in the unit cell parameter of a similar pentlandite when annealed for 5 months at 150 °C was noticed, with some cell contraction, possibly indicating the onset of ordering after 1 month. The nature of ordering in natural pentlandite remains unclear; the contraction of the unit cell parameter is not in itself an indication of Ni/Fe ordering in synthetic pentlandite. It should be noted that the cell contraction reported by Rajamani and Prewitt (1975) and Tsukimura (1989) are more consistent with ordering of Ni or Fe^{2+} in a low spin state onto the octahedral site. Clearly, however, whatever the form of the ordering, it takes place on a time scale longer than 2 months or at a lower temperature. Prolonged annealing experiments on the ^{60}Ni-pentlandite sample are currently underway at 100 °C, below the disordering temperature proposed by Tsukimura (1989) in an attempt to resolve this question.

TABLE 3. Thermal variations of distances (Å) and angles (degrees) in ^{60}Ni-pentlandite

T (°C)	25	225	300	25*
$[M(T)\text{-}M(T)]_e$	2.575	2.613	2.612	2.579
[M(O)-S]	2.436	2.425	2.456	2.430
$[M(T)\text{-}S]_1$	2.255	2.301	2.291	2.266
$[M(T)\text{-}S]_2$	2.147	2.156	2.170	2.152
<M(O)-S-M(T)>	126.2	126.6	126.3	126.4
$<M(T)\text{-}S\text{-}M(T)>_{e1}$	69.6	69.2	69.5	69.4
$<M(T)\text{-}S\text{-}M(T)>_{e2}$	107.7	106.9	107.5	107.2
$<M(T)\text{-}S\text{-}M(T)>_c$	109.471	109.471	109.471	109.471
$<S\text{-}M(T)\text{-}S>_1$	110.3	110.7	110.5	110.6
$<S\text{-}M(T)\text{-}S>_2$	108.6	108.2	108.5	108.3

Notes: M represents the metal (Fe or Ni). T stands for tetrahedra and O for octahedra. C and E indicate corner-shared or edge-shared tetrahedra, respectively (see Fig. 1). Since atomic parameters were fixed during the final cycles of refinement (for M distribution) errors are not given here.
* After an additional 2 months annealing at 150 °C.

Metal distribution in violarite

The neutron diffraction data collected at 25 and 225 °C and used in the structural refinement of violarite are shown in Figure 3. Thermal variations of unit cell and composition are summarized in Table 4, and atomic positions and isotropic thermal parameters are listed in Table 5. Although violarite is the dominant phase, with 76(1) wt% present at room temperature, some unreacted *mss* remains together with ~15 wt% pyrite formed during sulfation of the *mss*. Three sharp, but small, peaks at *d* ~2.10, 1.86, and 1.61 Å, that could not be indexed by any known phases, were excluded from the structure refinement. The composition of the ^{60}Ni-violarite is very close to the starting formula $FeNi_2S_4$ after refinement. Refinement of the distribution of Fe and Ni over the octahedral and tetrahedral sites showed that the latter was fully occupied by Ni and the octahedral site contains the Fe and the remaining Ni, giving an equal mixture of these metals on the site. Therefore, violarite has the inverse spinel structural type $(Fe^{2+},Ni^{3+})_O(Ni^{3+})_TS_4$. Heating the sample to 300 °C did not change the distribution of Fe and Ni over the tetrahedral and octahedral sites.

Thermal variations of interatomic distances and angles in ^{60}Ni-violarite are listed in Table 6. The shortest intermetallic distance M-M ~3.4 Å is between two octahedra. There are two

TABLE 4. Thermal variations of composition and structural parameters of ^{60}Ni-violarite

T (°C)	Formula	$wt\%_{violarite}$	a (Å)	$\%^{60}Ni(O)$	$\%^{60}Ni(T)$	$wt\%_{mss}$	$wt\%_{pyrite}$
25*	$Fe_{0.95}Ni_{2.05}S_4$	76(1)	9.4424(1)	54(2)	97(1)	*7(1)*	*17(1)*
75	$Fe_{1.04}Ni_{1.96}S_4$	74(1)	9.4452(1)	50(3)	97(1)	*8(1)*	*18(1)*
150	$Fe_{0.84}Ni_{2.16}S_4$	84(1)	9.4612(1)	59(3)	98(1)	*8(1)*	*8(1)*
225	$Fe_{1.00}Ni_{2.00}S_4$	77(1)	9.4709(1)	52(3)	97(1)	*8(1)*	*15(1)*
300	$Fe_{0.83}Ni_{2.17}S_4$	79(1)	9.4847(2)	59(6)	99(3)	*7(1)*	*14(1)*
25	$Fe_{1.14}Ni_{1.86}S_4$	76(1)	9.4498(1)	47(2)	93(1)	*7(1)*	*17(1)*
–73	$Fe_{1.19}Ni_{1.81}S_4$	72(1)	9.4318(1)	44(2)	93(1)	*9(1)*	*19(1)*
–173	$Fe_{1.19}Ni_{1.81}S_4$	72(1)	9.4211(1)	44(2)	92(1)	*9(1)*	*19(1)*

Note: Errors are noted in parentheses.
* *mss* [$P6_3/mmc$: a =3.4118(2) and c = 5.3715(4) Å] and pyrite [$Pa\bar{3}$: a = 5.4237(3) Å] with shared Fe/^{60}Ni occupancy on M site.

TABLE 5. Thermal variation of atom positions and displacement parameters in ^{60}Ni-violarite

T (°C)	$U_{iso}(M) \times 10^2$ (Å^2)	x(S) in 32e	$U_{iso}(S) \times 10^2$ (Å^2)
25	0.05(4)	0.2578(2)	0.43(9)
75	0.06(5)	0.2572(3)	0.35(14)
150	0.01(10)	0.2583(3)	0.25(15)
225	0.32(10)	0.2573(3)	0.33(15)
300	0.45(22)	0.2586(6)	1.01(34)
25	0.67(8)	0.2581(2)	0.43(12)
–73	0.11(5)	0.2573(2)	0.15(9)
–173	0.03(5)	0.2582(2)	0.16(6)

Note: Estimated standard deviations are given in parentheses.
x(M) = y(M) = z(M) = 0.125 : 8*a* Wyckoff position (Tetrahedral site) for $Fd\bar{3}\,m$ space group
x(M) = y(M) = z(M) = 0.5 : 4*f* (Octahedral site)
x(S) = y(S) = z(S) ~ 0.25 : 32*e*

TABLE 6. Thermal variations of distances (Å) and angles (degrees) in ^{60}Ni-violarite

T (°C)	25	75	150	225	300	25
[M(O)-S]	2.289(1)	2.295(2)	2.289(2)	2.301(2)	2.2935(3)	2.288(2)
[M(T)-S]	2.172(3)	2.163(4)	2.185(4)	2.170(4)	2.195(10)	2.179(3)
<M(O)-S-M(O)>	93.6(1)	93.4(1)	93.9(1)	93.4(1)	94.0(3)	93.8(1)
<M(O)-S-M(T)>	122.6(1)	122.8(1)	122.5(1)	122.8(1)	122.4(2)	122.5(1)
<S-M(O)-S>$_1$	86.2(1)	86.5(1)	86.0(1)	86.5(1)	85.9(3)	86.1(1)
<S-M(O)-S>$_2$	93.7(1)	93.5(1)	94.0(1)	93.5(1)	94.1(1)	93.9(1)
<S-M(T)-S>	109.471(1)	109.471(1)	109.471(1)	109.471(1)	109.471(2)	109.471(1)

Notes: Where M replaces the metal (Fe or Ni). T stands for tetrahedra and O for octahedra (see Fig. 1). Errors are given in parentheses.

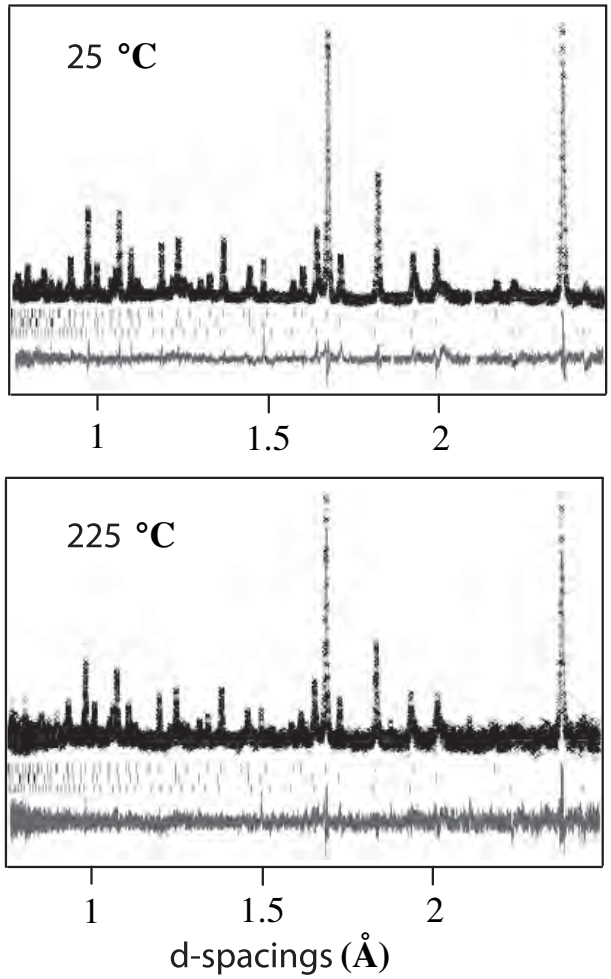

FIGURE 3. Observed (cross), calculated (weak line), and difference (strong bottom line) time-of-flight neutron diffraction patterns for ^{60}Ni-containing violarite at 25 °C (upper) and 225 °C (lower) using backscattering detectors (bank 1). Bragg peaks are represented by vertical lines: violarite (top), *mss* (middle), and pyrite (bottom). Goodness-of-fit parameters (R_p, R_{wp}, χ^2) are: 0.1543, 0.1740, 2.474 and 0.1522, 0.1730, 1.219 at 25 and 225 °C, respectively.

short M-S distances in the violarite structure, one for each polyhedral environment while there are two types of M-S-M angles and three different S-M-S angles varying with temperature. The M(O)-S distance of 2.289(1) Å at room temperature is significantly shorter than that observed in pentlandite and indicates the Fe^{2+} is in a low spin configuration. The site is shared with Ni^{3+}, probably in the same spin state. These findings are in accordance with the conclusions of Vaughan and Craig (1985). All M-S distances tend to increase slowly with temperature as the unit cell expands but return to their initial values when measured at room temperature after annealing; there is no irreversible thermal expansion in violarite or disordering upon heating, unlike in pentlandite. There is no indication of structural change or magnetic ordering in neutron diffraction patterns with lowering temperature down to –173°C.

Although both pentlandite and violarite are chemically similar and structurally derived from ccp arrays of S, the metal ions behave very differently, even when treated under similar thermal regimes. Violarite is fully ordered while pentlandite is difficult to order even with prolonged low temperature annealing; only in nature does it appear to order. One important difference between the structures in the metal-metal bonding in pentlandite; the M-M distances are 2.6 Å. There is no M-M bonding on violarite, the shortest M-M distance is ~3.4 Å. It is this intermetallic bonding that stabilizes the metal rich stoichiometry and possibly raises a kinetic barrier to metal ordering. Only when fully ordered synthetic pentlandite is prepared will the nature of this ordering process be fully understood.

ACKNOWLEDGMENTS

We thank Sandra Moussa and Haipeng Wang for their assistance with the data collection at ISIS. The constructive comments of the two anonymous referees help to improve the presentation of our results. We acknowledge the financial support of the Australian Research Council and the Australian Institute for Nuclear Science and Engineering.

REFERENCES CITED

Durazzo, A. and Taylor, L.A. (1982) Exsolution in the *Mss*-pentlandite system: Textural and genetic implications for Ni-sulfide ores. Mineralium Deposita, 17, 313–332.

Etschmann, B., Pring, A., Putnis, A., Grguric, B.A., and Studer, A. (2004) A kinetic study of the exsolution of pentlandite $(Ni,Fe)_9S_8$ from the monosulfide solid solution (Fe,Ni)S. American Mineralogist, 89, 39–50.

Fedorov, V.A., Kesler, Y.A. and Zhukov, E.G. (2003) Magnetic semiconducting chalcogenide spinels: preparation and physical chemistry. Inorganic Materials, 38, supplement no. 2, S68–S88.

Grguric, B.A. (2002) Hypogene violarite of exsolution origin from Mount Keith, Western Australia: field evidence for a stable pentlandite-violarite tie line. Mineralogical Magazine, 66, 313–326.

Ibberson, R.M., David, W.I.F., and Knight, K.S. (1992) The High Resolution Neutron Powder Diffractometer (HRPD) at ISIS—A User Guide <../documentation/HRPDguide/HRPDguideFramePage.htm> Report RAL-92-031.

Knop, O., Huang, C.-H., and Woodhams, F.W.D. (1970) Chaclogenides of the transition elements. VII. A Mössbauer study of pentlandite. American Mineralogist, 55, 1115–1130.

Misra, K.C. and Fleet, M.E. (1974) Chemical composition and stability of violarite. Economic Geology, 69, 391–403.

Naldrett, A.C., Craig, J.R., and Kullerud, G. (1967) The central portion of the Fe-Ni-S system and its bearing on pentlandite exsolution in iron-nickel sulfide ores. Economic Geology, 62, 826–847.

Nickel, E.H., Ross, J.R., and Thornber, M.R. (1974) The supergene alteration of pyrrhotite-pentlandite ore at Kambalda, Western Australia. Economic Geology, 69, 93–107.

Rajamani, V. and Prewitt, C.T. (1973) Crystal chemistry of natural pentlandites. Canadian Mineralogist, 12, 178–187.

——— (1975) Thermal expansion of the pentlandite structure. American Min-

eralogist, 60, 39–48.
Shannon, R.D. (1976) Revised effective ionic radii and systematic studies of interatomic distances in halides and chalcogenides. Acta Crystallographica A, 32, 751–767.
Tenailleau, C., Etschmann, B., Wang, H., Pring, A., Grguric, B.A., and Studer, A. (2005) Thermal expansion of troilite and pyrrhotite determined by in situ cooling (873 to 373 K) neutron powder diffraction measurements. Mineralogical Magazine, 69, 205–216.
Tenailleau, C., Pring, A., Etschmann, B., Brugger, J., Grguric, B.A., and Putnis, A. (2006) Transformation of pentlandite to violarite under mild hydrothermal conditions. American Mineralogist, 91, 706–709.
Townsend, M.G., Gosselin, J.R., Horwood, J.L., Ripley, L.G., and Tremblay, R.J. (1977) Violarite, a metallic natural spinel. Physica Status Solidi, 40, K25–29.
Tsukimura, K. (1989) Fe/Ni distribution in pentlandite at high temperature and the estimated pressure-temperature dependence of the distribution. Mineralogical Journal, 14, 323–337.
Tsukimura, K. and Nakazawa, H. (1984) Determination of Fe/Ni distribution in pentlandites Acta Crystallographica B40**,** 364–367.
Vaughan, D.J. and Craig, J.R. (1974) The crystal chemistry and magnetic properties of iron in the monosulfide solid solution of the Fe-Ni-S system. American Mineralogist, 59, 926–933.
——— (1985) The crystal chemistry of iron-nickel thiospinels. American Mineralogist, 70, 1036–1043.

MANUSCRIPT RECEIVED NOVEMBER 9, 2005
MANUSCRIPT ACCEPTED MAY 3, 2006
MANUSCRIPT HANDLED BY MARTIN KUNZ